Journal of Electronic Materials (2022) 51:2390–2395
https://doi.org/10.1007/s11664-022-09521-x

ORIGINAL RESEARCH ARTICLE

Influence of Substrate Temperature on Structure and Properties of Nb-Doped β-Ga_2O_3 Films

Ruidong Li[1,2] · Jinxiang Deng[1] · Le Kong[1] · Junhua Meng[1] · Juxin Luo[1] · Qing Zhang[1] · Hongli Gao[1] · Qianqian Yang[1] · Guisheng Wang[1] · Xiaolei Wang[1]

Received: 8 October 2021 / Accepted: 10 February 2022 / Published online: 1 March 2022

Abstract

Nb-doped β-Ga_2O_3 films were deposited on p-Si (100) and quartz substrates using radio frequency magnetron sputtering technology at various substrate temperatures. All the films annealed in an argon ambient. The surface morphology and crystal structure of the films were studied using atomic force microscope and x-ray diffraction technologies, and the results indicated that the film had a flat surface and a good crystal structure when the substrate temperature was 523 K. We investigated the optical properties of the samples, and the results highlight that Nb-doped β-Ga_2O_3 films exhibit high transmittance of above 80% to UV–visible light with a wavelength above 400 nm. Furthermore, the optical band gap of the Nb-doped β-Ga_2O_3 films decreases with increasing substrate temperature. The electrical characteristics show that the current is larger, and that the contact between the Ag electrode and the Nb-doped β-Ga_2O_3 film is an ohmic contact, when the substrate temperature is 523 K. All the results are beneficial for practical applications.

Keywords Nb-doped β-Ga_2O_3 film · substrate temperature · morphology and roughness · optical properties · electrical characteristics

Introduction

Solar irradiation between 200 nm and 280 nm, called the solar-blind region, does not reach the surface of the earth[1] because of the strong absorption of deep ultraviolet (UV) light by the stratospheric ozone. Since no interference sources exist, solar-blind UV detection provides superior advantages, such as lower false alarm rates and an all-weather work environment compared with infrared detection.[2,3] Recently, solar-blind solid photodetectors based on wide band gap semiconductors have attracted intensive attention.[4–9] Due to the ultra-wide band gap of Eg (4.7–4.9 eV), β-Ga_2O_3 is considered an ideal candidate for fabricating solar-blind photodetectors.[4,6,10] Many works have been carried out to prepare high-quality β-Ga_2O_3 films on various substrates using the optimization of processing technology.[11–15] However, because of the poor thermal and electrical conductivity of pure β-Ga_2O_3 films, which limits their application, many studies to improve the properties of β-Ga_2O_3 thin films using doping technology have emerged. To date, there have been several experiments and theoretical investigations of the properties of β-Ga_2O_3 films which are incorporated with various impurities.[16–25] Among them, Nb dopant has emerged as the best candidate for *n*-type doping because the atomic radius of Nb is very close to that of the Ga atom. To the best of our knowledge, however, there has been almost no research on the properties of Nb-doped β-Ga_2O_3 films prepared through experimental methods. Therefore, it is necessary to explore the properties of Nb-doped β-Ga_2O_3 films prepared under different temperatures.

There are several methods to grow the films, such as radio frequency (RF) magnetron sputtering, thermal evaporation, spin-coating, molecular beam epitaxy, and so on. RF magnetron sputtering technology has the advantages of simple operation, good film-forming quality, and stable performance. In addition, RF magnetron sputtering technology is suitable for semiconductor materials. Ga_2O_3 and Nb_2O_5

✉ Ruidong Li
liruidong_hit@163.com

✉ Jinxiang Deng
jdeng@bjut.edu.cn

[1] Faculty of Science, Beijing University of Technology, Beijing 100124, China

[2] Department of Basic Courses, Institute of Disaster Prevention, Hebei 065201, China

happen to be semiconductor materials. Therefore, in this paper, Nb-doped β-Ga_2O_3 thin films were grown on p-Si and quartz substrates under various temperatures by RF magnetron sputtering technology. The surface morphology and crystal structure of the Nb-doped β-Ga_2O_3 thin films have been researched. The optical properties and electrical characteristics of the films have also been investigated. This research will be helpful for the practical application of the thin films.

Experimental

Film Deposition

Nb-doped β-Ga_2O_3 films were directly deposited on p-type Si (100) and quartz substrates by RF magnetron sputtering under Ar ambient, with Ga_2O_3 (purity: 99.99%) and Nb_2O_5 targets (purity: 99.99%). Before depositing the films, the substrates were cleaned with methylbenzene, acetone, and ethyl alcohol for 15 min in sequence using an ultrasonic cleaner to remove organic contaminants. Then, they were cleaned with deionized water and dried in N_2 gas.

Before depositing the films, the p-type Si and quartz substrates were placed in the sputtering chamber. Pure Ga_2O_3 and Nb_2O_5 targets were used as the target. The distance between the substrate and target was ~35 mm. The chamber was evacuated to a base pressure of 5×10^{-4} Pa before sputtering. Ar (80 sccm) was introduced using mass flow controllers, and the working pressure in the chamber was kept at 1 Pa using a throttle valve. The RF power applied to the Ga_2O_3 and Nb_2O_5 target were 80 W and 40 W, respectively. Before depositing the films, the substrates were covered by a dam-board. When the substrates reached the set temperature, the target was presputtered for 10 min before formal sputtering. Then, the dam-board was removed to deposit the film. The substrates were rotated (~15 rpm) to make the films more uniform. The Nb-doped β-Ga_2O_3 films grew at various substrate temperatures (323 K, 423 K, 523 K, and 613 K), and all the films had the same thickness of 300 nm. All the samples were annealed for 4 h at 1173 K under Ar atmosphere.

Characterization of Films

Atomic force microscopy (AFM) examined the morphology and roughness of the samples after annealing. A Bruker D8 Advance x-ray diffraction (XRD) instrument equipped with Cu-Kα ($\lambda = 1.5406$ Å) radiation was used to investigate the crystal structure of the samples. In addition, the optical properties were analyzed using a UV–visible spectrophotometer (Shimadzu-3600) with a wavelength between 200 nm and 800 nm, while photoluminescence measurements were conducted using a fluorimeter (Horiba Jobin Yvon iHR550). To research the electrical characteristics, the current-to-voltage (*I–V*) characteristics were measured by a Keithley 4200-SCS semiconductor characterization system at room temperature and in the dark.

Results and Discussion

The surface morphology of Nb-doped β-Ga_2O_3 films prepared at various temperatures (323 K, 423 K, 523 K ,and 613 K) are investigated using AFM and are shown in Fig. 1. Figure 2 shows the root-mean-square (RMS) of the samples at different temperatures. From Fig. 2, the RMS roughness changes as the temperature increases. The RMS roughness of the samples was kept to a minimum and the surface morphology was the uniform at the temperature of 523 K, which indicates that the samples were in a nano-crystalline state.[26] The surface morphology of the samples was dense and relatively flat when the temperature was lower than 523 K. The atoms in the samples can migrate with increasing temperature, thereby making the samples more uniform, which helps their deposition.[27] The RMS values of the samples were 5.05 nm, 5.14 nm, 4.79 nm, and 6.60 nm when the temperatures were 323 K, 423 K, 523 K, and 613 K, respectively. The increase in the RMS value of the sample prepared at 613 K follows the co-effects of crystallization and high-temperature reconstruction. Enough energy increases the atom vibrations and movement, which finally transforms them into island-like structures at the temperature of 613 K, due to high-temperature reconstruction of the crystal structure driven by enhanced atomic migration and surface energy minimization.[28]

Figure 3 shows the XRD patterns for the samples prepared at various temperatures. Peaks appeared at 30°, 38°, 44°, and 65°, corresponding to the (400), (411), (202), and (300) planes of the Ga_2O_3 monoclinic phase, respectively, which suggests that beta Ga_2O_3 was formed. Figure 4a shows the peak position, full width at half-maximum (FWHM), and intensity of the (400) peak. From the Bragg equation:

$$2d \sin\theta = n\lambda$$

where n is the order of diffraction and d is the distance of the lattice plane, when the temperature increases, the peak position moves to a small angle, indicating that the crystallite size becomes larger. Figure 4b shows the crystalline grain size and dislocation density. The crystallite size (D) of the sample is estimated using the Debye–Scherrer formula:

$$D = \frac{0.9\lambda}{\beta \cos\theta}$$

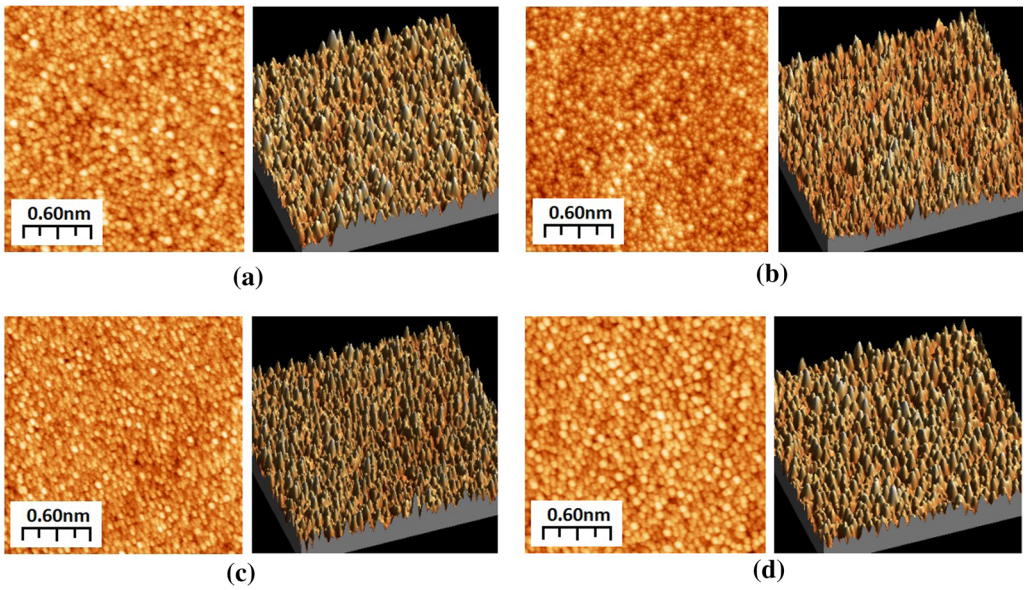

Fig. 1 2D and 3D AFM images of the samples at different temperatures (scan areas are 3 μm × 3 μm): (a) 323 K; (b) 423 K; (c) 523 K; (d) 613 K.

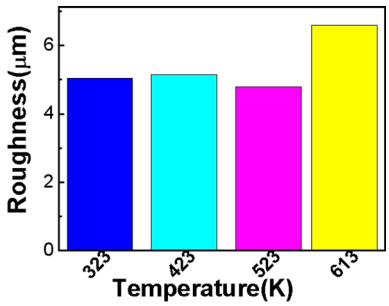

Fig. 2 RMS image of the samples at different temperatures.

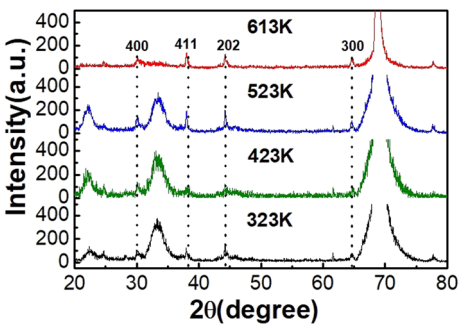

Fig. 3 XRD patterns of the films at various temperatures.

, where λ (= 0.154 nm) is the wavelength of the x-ray radiation used, β is the width of the (400) peak at half maximum in radians, and θ is Bragg's diffraction angle. The results obtained from Bragg's equation and the Debye–Scherrer

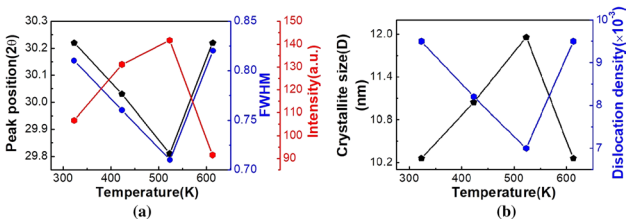

Fig. 4 XRD variation of (a) peak position, FWHM, and intensity; (b) crystallite size and dislocation density.

formula agree well with the results of AFM. The dislocation density (δ) represents the extent of defects in the sample due to the imperfections in the crystal following the mismatch of lattices. This can be calculated using the relationship,

$$\delta = \frac{1}{D^2}$$

where D is the crystallite size. The increase in the intensity of the crystalline peaks is directly proportional to the increase in temperature, indicating the improvement of the sample crystal quality.

The optical properties of the Nb-doped β-Ga_2O_3 have been investigated by a UV–visible spectrophotometer. The transmittance spectra of the samples as a function of wavelength in the range of 200–800 nm for the samples prepared at various temperatures (323 K, 423 K, 523 K, and 613 K) are presented in Fig. 5a. All the samples showed high transmittance of above 80% to UV–visible light with a wavelength above 400 nm. The optical band gap (E_g) is an important optical parameter for operating an optoelectronic

device. As a direct electron transition semiconductor for Nb-doped β-Ga_2O_3, the optical band gap is calculated from the fundamental absorption edge of the samples using the Tauc equation[29]:

$$\alpha h\nu = \left(h\nu - E_g\right)^{1/2}$$

where C is a constant, h is Planck's constant, and ν is the frequency. The absorption coefficient, α, is calculated from the transmission spectrum using the relationship, $\alpha = (\ln 1/T)/t$, where T is the transmittance and t is the thickness of the film. From the Tauc equation, if $\alpha h\nu$ is zero, $h\nu$ becomes equal to E_g. The optical band gap of the samples prepared at various temperatures is determined by the linear extrapolation of $(\alpha h\nu)^2$ against $h\nu$ plot.[30] Figure 5b shows typical variations of $(\alpha h\nu)^2$ versus $h\nu$ for Nb-doped β-Ga_2O_3 films with different temperatures. Figure 6 shows the relationship between the optical band gap and the substrate temperature. These data show that the optical band gap decreases from a value of 4.87 eV for the sample deposited at 323 K to 4.83 eV for the sample deposited at 613 K. The decrease in the optical energy gap can be attributed to the influence of different factors, including grain size, the preparing environment, carrier concentration, or deviation from the stoichiometry of the film, and so on.[31] The values of the optical band gap are higher at lower temperatures due to excess O_2 or the amorphous states.[32,33] The values of the optical band gap decrease with an increase in the temperature and is usually caused by a shift in energy of the valence and conduction bands resulting from some known effect, such as electron–impurity and electron–electron scattering.[34] This indicates that the crystalline state is better and increases the carrier concentration.

As an essential approach to studying the defect level emissions in semiconducting oxides, photoluminescence spectroscopy is measured. Figure 7 shows the photoluminescence spectra of Nb-doped β-Ga_2O_3 films recorded using a fluorimeter for which the excitation wavelength is 325 nm (~3.82 eV). The optical band gaps for β-Ga_2O_3 and Nb_2O_5 are 4.9 eV[35–37] and 3.58 eV,[38] respectively. From Fig. 7, the peak position is ~495 nm (~2.51 eV) [except the film prepared at 613 K (~525 nm, 2.38 eV)], indicating that it is not the intrinsic transition of β-Ga_2O_3 and Nb_2O_5. Figure 7 also shows that the defect-related luminescence spectra of Nb-doped β-Ga_2O_3 films are in the blue light region due to the sample's intrinsic defects, such as oxygen vacancy (V_O) and gallium vacancy (V_{Ga}), or the gallium–oxygen vacancy pairs complex ($V_O - V_{Ga}$).[39–41] Furthermore, from Fig. 7, the peak position of the blue light showed a blue shift with an increase in temperature (except at 613 K). This band gap widening may be explained by the Burstein–Moss shift.[42] Photoluminescence studies of the samples led to semi-insulating samples with sub-band gap emission bands close to 2.51 eV and 2.38 eV when the temperature was 613 K. This shows that the deep level may have formed when Nb-doped β-Ga_2O_3. These peak positions correspond to two states at energy levels of E_c—2.51 eV and —2.38 eV, respectively, corresponding to the electron emission processes from each of the two deep states to the conduction band in β-Ga_2O_3.[43] Further research is needed on the defect types. Photoluminescence intensity decreases with increasing temperature.

To understand the effects of temperature on Nb-doped β-Ga_2O_3 films, silver was deposited on the films as an electrical contact. Figure 8a and b shows the structure and the *I–V* characteristics of the Nb-doped β-Ga_2O_3 films in the air prepared under various temperatures. The *I–V* characteristics

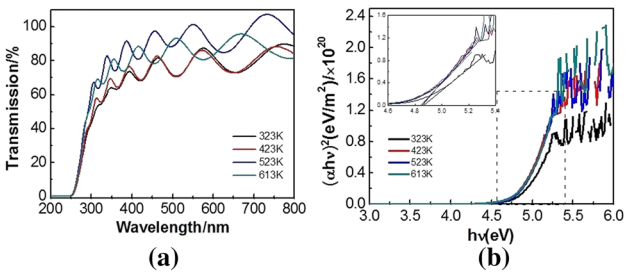

Fig. 5 Transmittance spectra (a) and Tauc plot (b) of Nb-doped β-Ga_2O_3 film prepared at various temperatures.

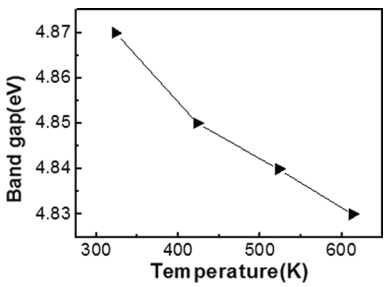

Fig. 6 The relationship between the optical band gap and temperature.

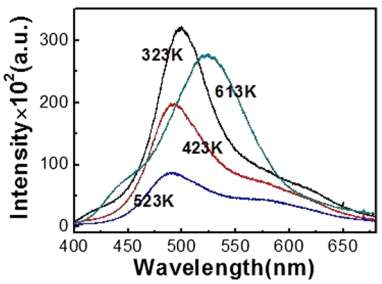

Fig. 7 Photoluminescence spectra of Nb-doped β-Ga_2O_3 thin films at various temperatures.

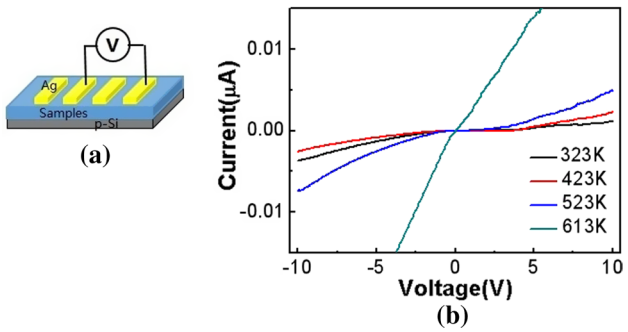

Fig. 8 (a) Schematic of the structure, (b) the *I–V* characteristics of the Nb-doped β-Ga_2O_3 films prepared at various temperatures.

show a rectifying behavior. Figure 8b shows the *I–V* curves at various temperatures (323 K, 423 K, 523 K, and 613 K). It follows that the current of the film increases with increasing temperature. The contact between the electrode and the samples is almost an ohmic contact when the temperature is 523 K, which is helpful in practical applications. However, for the temperature at 613 K, the current increases linearly with the increase in voltage, thereby affecting the sample structures. At 613 K, because of the high-temperature reconstruction of the crystal structure driven by enhanced atomic migration and surface energy minimization,[28] the large crystalline grain is transformed into island-like structures, leading to increased roughness. With the films growing, the grain boundary becomes smaller, decreasing the electrical resistivity between the metal electrode and the sample. Therefore, it will serve as a good electric conductor with an increased temperature.

Conclusions

Nb-doped β-Ga_2O_3 films were grown under various substrate temperatures using RF sputtering technology. The dependence of the structural and morphological properties of Nb-doped β-Ga_2O_3 films on their preparation temperature was studied. Furthermore, the influence of the temperature of the substrate on the optical and electrical properties of the films was investigated. All the films grown under different temperatures were crystalline. The intensity of the (400) and (300) peaks increased gradually with increased temperature. The average transmittance of the Nb-doped β-Ga_2O_3 films in the visible region was above 80% and the band gap decreased with increasing temperature. The Nb-doped β-Ga_2O_3 films showed rectifying-type *I–V* characteristics. With the increase in temperature, the contact between the Ag electrode and the samples tended to have ohmic contact. The results demonstrate that Nb-doped β-Ga_2O_3 films have several practical applications.

Acknowledgments This work is supported by the Natural Science Foundation of Beijing City, China (Grant No. 4192016), the Natural Science Foundation of Beijing City, China (Grant No. 4102014) and the Funding for the Development Project of Beijing Municipal Education Commission of Science and Technology (Grant No. KZ201410005008).

Conflict of interest This manuscript has not been published elsewhere and is not under consideration by another journal. We have approved the manuscript and agree with submission to *Journal of Electronic Materials*. There are no conflicts of interest to declare.

References

1. M. Razeghi and A. Rogalski, Semiconductor ultraviolet detectors. *J. Appl. Phys.* 79, 7433 (1996).
2. A. Malik, A. Seco, E. Fortunato, and R. Martins, New UV-enhanced solar blind optical sensors based on monocrystalline zinc sulphide. *Sens. Actu. A* 67, 68 (1998).
3. L. Li, E. Auer, M. Liao, X.S. Fang, T.Y. Zhai, U.K. Gautam, A. Lugstein, Y. Koide, Y. Bando, and D. Golberg, Deep-ultraviolet solar-blind photoconductivity of individual gallium oxide nanobelts. *Nanoscale* 3, 1120 (2011).
4. R. Suzuki, S. Nakagomi, and Y. Kokubun, Solar-blind photodiodes composed of a Au Schottky contact and a β-Ga_2O_3 single crystal with a high resistivity cap layer. *Appl. Phys. Lett.* 98, 1114 (2011).
5. Z.D. Huang, W.Y. Weng, S.J. Chang, C.J. Chiu, T.-J. Hsueh, and S.-L. Wu, AlGaN/GaN heterostructure ultraviolet three-band photodetector. *IEEE Sens. J.* 13, 3462 (2013).
6. T. Oshima, T. Okuno, N. Arai, N. Suzuki, S. Ohira, and S. Fujita, Vertical solar-blind deep-ultraviolet Schottky photodetectors based on β-Ga_2O_3 substrates. *Appl. Phys. Express* 1, 011202 (2008).
7. M. Razeghi, Short-wavelength solar-blind detectors-status, prospects, and markets. *Proc. IEEE* 2002, 1006 (2002).
8. X. Du, Z. Mei, Z. Liu, Y. Guo, T. Zhang, Y. Hou, Z. Zhang, Q. Xue, and A.Y. Kuznetsov, Controlled growth of high-quality ZnO-based films and fabrication of visible-blind and solar-blind ultra-violet detectors. *Adv. Mater.* 21, 4625 (2009).
9. W. Weng, T. Hsueh, S. Chang, G. Huang, and H. Hsueh, A β-Ga_2O_3/GaN Schottky barrier photodetector. *IEEE Photon. Technol. Lett.* 23, 444 (2011).
10. Y. Kokubun, K. Miura, F. Endo, and S. Nakagomi, Sol-gel prepared β-Ga_2O_3 thin films for ultraviolet photodetectors. *Appl. Phys. Lett.* 90, 031912 (2007).
11. G. Sinha, K. Adhikary, and S. Chaudhuri, Sol-gel derived phase pure α-Ga_2O_3 nanocrystalline thin film and its optical properties. *J. Cryst. Growth* 276, 204 (2005).
12. Z. Ji, J. Du, J. Fan, and W. Wang, Gallium oxide films for filter and solar-blind UV detector. *Opt. Mater.* 28, 415 (2006).
13. M. Fleischer, W. Hanrieder, and H. Meixner, Stability of semiconducting gallium oxide thin films. *Thin Solid Films* 190, 93 (1990).
14. Y. Lv, J. Ma, W. Mi, C. Luan, Z. Zhu, and H. Xiao, Characterization of β -Ga_2O_3 thin films on sapphire (0001) using metal-organic chemical vapor deposition technique. *Vacuum* 86, 1850 (2012).
15. T. Oshima, T. Okuno, and S. Fujita, Ga_2O_3 thin film growth on c-plane sapphire substrates by molecular beam epitaxy for deep-ultraviolet photodetectors. *Jpn. J. Appl. Phys.* 46, 7217 (2007).

16. Z.P. Wu, G.X. Bai, Q.R. Hu, D.Y. Guo, C.L. Sun, L.Y. Ji, M. Lei, L.H. Li, P.G. Li, J.H. Hao, and W.H. Tang, Effects of dopant concentration on structural and near-infrared luminescence of Nd^{3+}-doped beta-Ga_2O_3 thin films. *Appl. Phys. Lett.* 106, 171910 (2015).
17. W. Mi, X.J. Du, C.N. Luan, H.D. Xiao, and J. Ma, Electrical and optical characterizations of β-Ga_2O_3: Sn films deposited on MgO (110) substrate by MOCVD. *RSC Adv.* 4, 30579 (2014).
18. F.B. Zhang, K. Saito, T. Tanaka, M. Nishio, and Q.X. Guo, Electrical properties of Si doped Ga_2O_3 films grown by pulsed laser deposition. *J. Mater. Sci. Mater. Electron.* 26, 9624 (2015).
19. B.K. Kang, S.R. Mang, H.D. Lim, K.M. Song, Y.H. Song, D.H. Go, M.K. Jung, K. Senthil, and D.H. Yoon, Synthesis, morphology and optical properties of pure and Eu^{3+} doped β-Ga_2O_3 hollow nanostructures by hydrothermal method. *Mater. Chem. Phys.* 147, 178 (2014).
20. W.H. Li, Y.K. Peng, C. Wang, X.L. Zhao, Y.S. Zhi, H. Yan, L.H. Li, P.G. Li, H.J. Yang, Z.P. Wu, and W.H. Tang, Structural, optical and photoluminescence properties of Pr-doped beta-Ga_2O_3 thin films. *J. Alloy. Comp.* 697, 388 (2017).
21. A.A. Dakhel, Structural, optical, and opto-dielectric properties of W-doped Ga_2O_3 thin films. *J. Mater. Sci.* 47, 3034 (2012).
22. X.H. Wang, F.B. Zhang, K. Saito, T. Tanaka, M. Nishio, and Q.X. Guo, Electrical properties and emission mechanisms of Zn-doped β-Ga_2O_3 films. *J. Phys. Chem. Solid.* 75, 1201 (2014).
23. X.J. Feng, Z. Li, W. Mi, and J. Ma, Effect of annealing on the properties of Ga_2O_3: Mg films prepared on α-Al_2O_3 (0001) by MOCVD. *Vacuum* 124, 101 (2016).
24. H. Zhang, J.X. Deng, Z.W. Pan, Z.Y. Bai, L. Kong, and J.Y. Wang, Structural and optical properties of Nb-doped β-Ga_2O_3 thin films deposited by RF magnetron sputtering. *Vacuum* 146, 93 (2017).
25. H. Peelaers, and C.G. Van de Walle, Doping of Ga_2O_3 with transition metals. *Phys. Rev. B* 94, 195203 (2016).
26. F. Shi, J. Han, Y. Xing, J. Li, L. Zhang, T. He, T. Li, X. Deng, X. Zhang, and B. Zhang, Annealing effects on properties of Ga_2O_3 films deposited by plasma-enhanced atomic layer deposition. *Mater. Lett.* 237, 105 (2019).
27. H. Shen, Y. Yin, K. Tian, K. Baskaran, L. Duan, X. Zhao, and A. Tiwari, Growth and characterization of β-Ga_2O_3 thin films by sol-gel method for fast-response solar-blind ultraviolet photodetectors. *J. Alloys Compd.* 766, 601 (2018).
28. L.X. Qian, Y. Wang, Z.H. Wu, T. Sheng, and X.Z. Liu, β-Ga_2O_3 solar-blind deep-ultraviolet photodetector based on annealed sapphire substrate. *Vacuum* 140, 106 (2017).
29. H. Shen, X. Zhao, L. Duan, R. Liu, H. Li, and B. Wang, Effect of Na_{Zn}/Na_i ratio on structural, optical, and electrical properties of Na-doped ZnO thin films. *J. Appl. Phys.* 121, 155303 (2017).
30. G.C. Xie, L. Fang, L.P. Peng, G.B. Liu, H.B. Ruan, F. Wu, and C.Y. Kong, Effect of In-doping on the optical constants of ZnO thin films. *Phys. Procedia* 32, 651 (2012).
31. K.G. Saw, N.M. Aznan, F.K. Yam, S.S. Ng, and S.Y. Pung, New insights on the Burstein-Moss shift and band gap narrowing in indium-doped zinc oxide thin films. *PLoS ONE* 10, 0141180 (2015).
32. E. Vega, S.B. Isukapati, and T.N. Oder, Microstructure and optical properties of sputter-deposited Ga_2O_3 films. *J. Vacuum Sci. Technol. A* 39, 033412 (2021).
33. S.S. Kumar, E.J. Rubio, M.N. Alam, G. Martinez, S. Manandhar, V. Shutthanandan, S. Thevuthasan, and C.V. Ramana, Structure, morphology, and optical properties of amorphous and nanocrystalline gallium oxide thin films. *J. Phys. Chem. C* 117, 4194 (2013).
34. I. Hamberg, and C.G. Granvist, Evaporated Sn-doped In_2O_3 films: Basic optical properties and applications to energy-efficient windows. *J. Appl. Phys.* 60, 123 (1986).
35. D.Y. Guo, Z.P. Wu, Y.H. An, X.C. Guo, X.L. Chu, C.L. Sun, L.H. Li, P.G. Li, and W.H. Tang, Oxygen vacancy tuned Ohmic-Schottky conversion for enhanced performance in β-Ga_2O_3 solar-blind ultraviolet photodetectors. *Appl. Phys. Lett.* 105, 023507 (2014).
36. D.Y. Guo, Z.P. Wu, P.G. Li, Y.H. An, H. Liu, X.C. Guo, H. Yan, G.F. Wang, C.L. Sun, L.H. Li, and W.H. Tang, Fabrication of β-Ga_2O_3 thin films and solar-blind photodetectors by laser MBE technology. *Opt. Mater. Express* 4, 1067 (2014).
37. S. Nakagomi, T. Momo, S. Takahashi, and Y. Kokubun, Deep ultraviolet photodiodes based on β-Ga_2O_3/SiC heterojunction. *Appl. Phys. Lett.* 103, 072105 (2013).
38. S. Venkataraj, R. Drese, C. Liesch, O. Kappertz, R. Jayavel, and M. Wuttig, Temperature stability of sputtered niobium–oxide films. *J. Appl. Phys.* 91, 4863 (2002).
39. L. Binet, and D. Gourier, Origin of the blue luminescence of β–Ga_2O_3. *J. Phys. Chem. Solids* 59, 1241 (1998).
40. F. Kellendonk and T. Harwig, Some observations on the photoluminescence of doped β-galliumsesquioxide. *J. Solid State Chem.* 24, 255 (1978).
41. T. Onuma, S. Fujioka, T. Yamaguchi, M. Higashiwaki, K. Sasaki, T. Masui, and T. Honda, Correlation between blue luminescence intensity and resistivity in β-Ga_2O_3 single crystals. *Appl. Phys. Lett.* 103, 41910 (2013).
42. S.W. Xue, X.T. Zu, W.G. Zheng, H.X. Deng, and X. Xiang, Effects of annealing and dopant concentration on the optical characteristics of ZnO: Al thin films by sol–gel technique. *Physica B* 382, 201 (2006).
43. Z. Zhang, E. Farzana, A.R. Arehart, and S.A. Ringel, Deep level defects throughout the bandgap of (010) β-Ga_2O_3 detected by optically and thermally stimulated defect spectroscopy. *Appl. Phys. Lett.* 108, 052105 (2016).